

EXPLOITING SPATIAL INFORMATION WITH THE INFORMED COMPLEX-VALUED SPATIAL AUTOENCODER FOR TARGET SPEAKER EXTRACTION

Annika Briegleb

Mhd Modar Halimeh*

Walter Kellermann

Friedrich-Alexander-Universität Erlangen-Nürnberg, Erlangen, Germany
 {annika.briegleb, mhd.m.halimeh, walter.kellermann}@fau.de

ABSTRACT

In conventional multichannel audio signal enhancement, spatial and spectral filtering are often performed sequentially. In contrast, it has been shown that for neural spatial filtering a joint approach of spectro-spatial filtering is more beneficial. In this contribution, we investigate the influence of the training target on the spatial selectivity of such a time-varying spectro-spatial filter. We extend the recently proposed complex-valued spatial autoencoder (COSPA) for target speaker extraction by leveraging its interpretable structure and purposefully informing the network of the target speaker's position. Consequently, this approach uses a multichannel complex-valued neural network architecture that is capable of processing spatial and spectral information rendering informed COSPA (iCOSPA) an effective neural spatial filtering method. We train iCOSPA for several training targets that enforce different amounts of spatial processing and analyze the network's spatial filtering capacity. We find that the proposed architecture is indeed capable of learning different spatial selectivity patterns to attain the different training targets.

Index Terms— target speaker extraction, spectro-spatial filtering, training targets

1. INTRODUCTION

While neural networks have been the state of the art for single-channel audio signal enhancement for some time now, they are only recently moving into the focus for multichannel audio signal enhancement and, hence, spatial filtering. There have been several approaches to guide spatial filters, i.e., beamformers, by estimating intermediate entities by neural networks [1–5]. Other approaches emulate a beamformer by estimating its weights by a neural network [6–10] or replace the beamforming process by a neural network that directly estimates the clean speech signal [11, 12]. The first approach stays with the conventional definitions of beamformers, whereas the second and third approach exploit the nonlinear processing performed by the neural network and are denoted as neural spatial filters. While in conventional spatial filtering, spatial and spectral filtering are often performed sequentially, it was shown in [13, 14] that for neural spatial filtering joint spatial and spectral processing is more effective. In this paper, we focus on those neural spectro-spatial filters that estimate the beamformer weights by a neural network. For a deeper understanding of joint spectro-spatial filtering, we investigate how spatial information is exploited by a neural spectro-spatial filter. In [6], it has been shown that the Complex-valued Spatial Autoencoder (COSPA) learns a spatial selectivity pattern based on a target signal that was filtered by a minimum variance

distortionless response-beamformer (MVDR BF). In this paper, we examine how the target signal used for training affects the capability of a neural spectro-spatial filter to perform spatial filtering. To this end, we consider the problem of target speaker extraction (TSE) from a mixture of speakers and extend COSPA by informing it about the target speaker's direction of arrival (DoA) (cf. Sec. 2.1). We then discuss different target signals for training the network and their relation to spatial processing in Sec. 2.2. In Sec. 3.1, we detail our experimental setup and present and discuss the corresponding results in Sec. 3.2. Sec. 4 concludes the paper.

2. PROVIDING SPATIAL INFORMATION FOR COSPA

In the following, we briefly introduce the COSPA framework and explain how it is modified to exploit spatial information for TSE (Sec. 2.1). A discussion on the spatial selectivity conveyed by appropriate target signals for multichannel processing follows in Sec. 2.2.

2.1. Extension of COSPA

We consider a signal with M microphone channels, captured by an arbitrary microphone array, where the signal at microphone m in time-frequency bin (τ, f) is given by

$$X_m(\tau, f) = D_m(\tau, f) + \sum_{i=1}^I U_{im}(\tau, f) + N_m(\tau, f). \quad (1)$$

$D_m(\tau, f) = H_m^*(\tau, f)S(\tau, f)$ denotes the desired speaker's signal at microphone m based on the acoustic transfer function $H_m(\tau, f)$ from the desired speaker to the m -th microphone. U_{im} denotes the contribution of interfering speaker i , $i = 1, \dots, I$, at microphone m and N_m is additional low-level sensor noise. The goal is to suppress the interfering speakers and to extract the source signal S , or a reverberant image of it, with minimal distortions. Thus, dereverberation is not explicitly addressed in this paper. We allow different target speakers and speaker positions across utterances but assume that the speakers' identities and positions remain static within one utterance.

In [6], COSPA was introduced for multichannel denoising. This framework consists of an *encoder*, which, using a subnetwork denoted by $\mathbb{C}RUNet$, estimates a single-channel mask that is applied to all input channels and subsequently includes feature compression, a *comparator* which provides multichannel processing, and a *decoder* which outputs a mask \mathcal{M}_m for each channel. In this paper, we modify COSPA to the problem of TSE by adding DoA information.

2.1.1. Incorporating DoA information

For reliable TSE, the network needs to be informed about which speaker is the target speaker. This can be achieved by feeding characterizing (instantaneous) information about the target speaker into

*M. M. Halimeh is now with Fraunhofer Institute for Integrated Circuits IIS, Am Wolfsmantel 33, 91058 Erlangen, Germany.

This work has been submitted to IEEE ICASSP 2023.

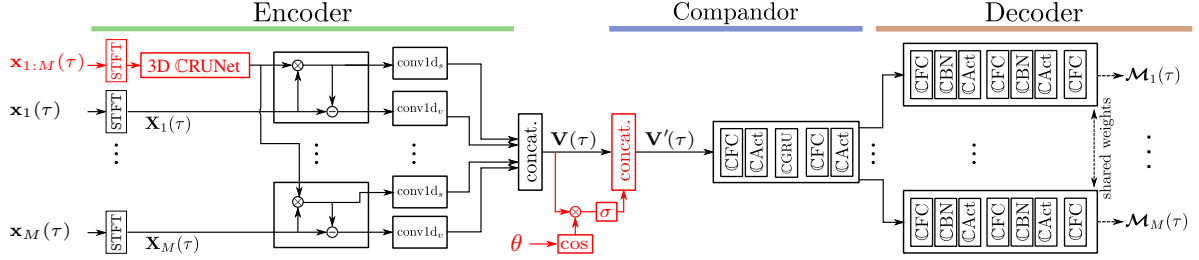


Fig. 1: Architecture of iCOSPAs (adapted from [6]). Differences to COSPA are marked in red.

the network for guidance. This can either be positional, i.e., DoA, information [15, 16], or identity information such as an adaptation utterance spoken by the target speaker [17–20]. The feature extraction involved in using an adaptation utterance for guidance is usually realized by an auxiliary neural network (e.g., [17]), which significantly increases the size of the overall neural network, while features based on DoA information can often be extracted without a neural network (e.g., [15]). Furthermore, in this paper, we want to focus on the spatial filtering aspect of COSPA, for which the DoA information is expected to be more relevant than the speaker identity. Considering these aspects and methods from literature, we find that exploiting DoA information and adding it to the network using scaled activations [17] works well for COSPA and also keeps the computational overhead small. Therefore, as depicted in Fig. 1, for the proposed *informed COSPA* (iCOSPAs) we scale the encoder output \mathbf{V} by the cosine of the DoA θ relative to the microphone array axis, pass it through a sigmoid activation function σ and append it to the original vector \mathbf{V} to obtain vector \mathbf{V}' , which is the input of the compandor. This differs from [17] as the original features are preserved. We add the guiding signal path before the compandor as it is the only part of COSPA that can process the different channels differently and where the DoA information can be beneficially used to increase the spatial selectivity. Given the many proven methods for DoA estimation in literature [21, 22], we assume that the utterance-wise DoA of the target speech is available with sufficient precision. The proposed approach doubles the size of the input of the first compandor layer but does not add other trainable parameters.

2.1.2. 3D convolutional layer for multichannel processing

In order to leverage multichannel information in the encoder, we use all channels to compute the single-channel mask in the encoder. We replace the complex-valued two-dimensional (2D) convolutions in the CRUNet of COSPA [6], which operate along the time and the frequency axis of the input signal, by complex-valued three-dimensional (3D) convolutions, which additionally extract features across all input channels. Real-valued 3D convolutional layers have been used in biomedical and video signal processing [23, 24], but not in audio signal processing. In the case of multichannel audio signal processing, extracting features across all three dimensions of the input tensor is intuitively beneficial as information about the spatial setup of the acoustic scene is encoded in the phase differences of the signals captured by the different channels, which also calls for complex-valued networks when operating in the time-frequency domain. Due to the relatively small kernel sizes of convolutional layers, replacing the 2D convolutions by 3D convolutions does not increase the size of the network significantly (cf. Table 1).

2.2. Training targets for spectro-spatial filtering

For joint spectro-spatial filtering with neural networks, several training targets, notably the clean source signal at the first microphone

[7], the time-aligned dry clean source signal [13], and an MVDR BF-filtered version of the source signal at the microphones [6] have been used in the literature. Further potentially advantageous target signals can be obtained by processing the clean reverberated signal with other beamformers, e.g., a simple delay-and-sum beamformer (DSB) to align the time of arrival of the microphone channels, or by modifying the source image at the microphone otherwise (e.g., removing the late reverberation). To obtain any of these targets, the network has to reflect different spatial and spectral filters. For the dry source signal, dereverberation has to be achieved additionally to spatial filtering, while the beamformer-filtered signals tolerate certain amounts of reverberation. To estimate the source image at the first microphone, the network has to implicitly estimate relative transfer functions. Therefore, the choice of the training target is expected to have a significant impact on the spectro-spatial filtering patterns learned by the network.

In the following, we experimentally investigate the spatial filtering behavior of iCOSPAs when guided by the additional DoA information. Furthermore, it is investigated how the training target influences the spatial filtering capacity of iCOSPAs. We consider as target signal options: the MVDR BF-filtered reverberant source signal, the DSB-filtered reverberant source signal, the reverberant source signal as captured by the first microphone (adding a small delay to avoid a theoretically possible need for noncausal processing), and the dry source signal, which was time-aligned with the signal at the first microphone.

3. EXPERIMENTAL VALIDATION

To verify the capabilities of iCOSPAs, we perform experiments on TSE. We describe the experimental setup in Sec. 3.1 and present and discuss the results in Sec. 3.2.

3.1. Setup and evaluation metrics

In our experiments, we consider scenarios with three speakers, for which we generate 6000 training samples of 7 s length, resulting in 11.7 h of training data. For each scenario, the room dimensions (in the range of [4-8, 4-8, 1-4] m), the reverberation time (0.2-0.5 s), and the positions of the speakers and the microphone array are sampled randomly. We use a uniform linear array with 3 microphones and a microphone distance of 4 cm. The target speaker is positioned 0.3-1.5 m from the array and has at least 10° angular distance to the interferers to both sides. Each source signal is convolved with its corresponding room impulse response generated by the image method [25] and the interferers are scaled such that the target-to-interferer ratio ranges from -5 to 5 dB. White noise is added to the mixture signal at a signal-to-noise ratio of 30-60 dB. The speech signals are taken from the TIMIT database [26] and are sampled at 16 kHz. For testing, we create 200 samples with speakers disjoint from the training dataset and keep the same settings as for training.

For the evaluation in Table 1, the test set is split into two subsets: Subset *cs* contains the 182 samples where COSPA extracts the desired speaker correctly, and Subset *ws* contains the 18 samples for which COSPA extracts the wrong speaker or does not separate the speakers at all (cf. Sec. 3.2.1).

In the following, we use the names COSPA and iCOSPA to discuss aspects of general relevance to the networks and use the MVDR BF-filtered source signal as target if not indicated otherwise. We append *-mvdr/dsb/mic1/dry* to the name when discussing the networks trained on specific targets. For the mic1-target experiments, the estimated mask for each channel is constrained to a maximum magnitude of $1/M$ to ensure that the network does not collapse into a single-channel method. We assume the 3D convolutional layer in the CRUNet of iCOSPA to be the default setting and append *-2D* when discussing iCOSPA with the 2D CRUNet.

We use the same hyperparameter and training settings for both COSPA and iCOSPA as in [6], with the exception of the additional convolutional kernels of size $\{2, 2, 1, 1\}$ along the channel axis in the four modules of iCOSPA’s CRUNet. Furthermore, the input of iCOSPA’s compandor is twice the size of that of COSPA due to the added DoA information. We use signal frames of length 1024 with a shift of 512 samples. In Sec. 3.2, we show beampatterns for COSPA and iCOSPA that were generated as described in [6].

As baseline methods, we provide results from an oracle MVDR BF, denoted as OMVDR BF, as described in [6], and results from the Embedding and Beamforming Network (EaBNet) introduced in [7] as a different neural spectro-spatial filter. We keep the settings of the EaBNet, including the frame length of 320 samples and the first microphone training target, as published without using an extra postfilter and train and test the network on our own dataset. All network sizes are given in Table 1.

The performance of the methods is measured by Perceptual Evaluation of Speech Quality (PESQ) [27], extended Short-Time Objective Intelligibility (ESTOI) [28] and the signal-to-interference ratio (SIR) [29]. We provide the performance metrics as the difference between metrics of the estimated signal and metrics of the mixture signal at the first microphone averaged over the test set. The discussion of which target to use for training, also raises the question which reference signal to use to compute the objective evaluation metrics. Here, we present the evaluation metrics based on both the dry source signal and the source image at the first microphone as reference to illustrate how the presence or absence of reverberation in the reference signal affects the performance metrics for different target signals. Both signals are time-aligned with the estimate.

3.2. Results and Discussion

We split the presentation of the results into two parts: In Sec. 3.2.1, we show the TSE performance of iCOSPA compared to COSPA and other baselines. In Sec. 3.2.2, we discuss the influence of the training targets introduced in Sec. 2.2 on the spatial selectivity of iCOSPA.

3.2.1. Performance evaluation

In Table 1, we present Δ PESQ, Δ ESTOI and Δ SIR for all methods introduced in Sec. 3.1. It can be seen that iCOSPA outperforms COSPA consistently for all targets. In Fig. 2, exemplary beampatterns for COSPA and iCOSPA are depicted, which show that iCOSPA reliably extracts the target speaker even in challenging spatial setups. As COSPA cannot know which speaker is the desired speaker for extraction, we exemplarily differentiate between the *cs* and *ws* subsets for the methods trained on the MVDR BF-filtered

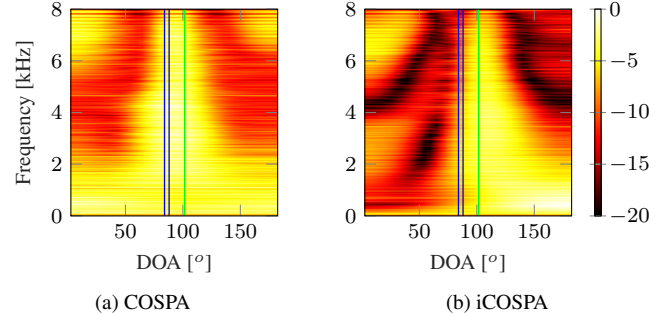


Fig. 2: Exemplary beampatterns for COSPA-mvdr and iCOSPA-mvdr. green line: target speaker; blue lines: interferers

target as described in Sec. 3.1. The scenarios in the *ws* subset are mainly characterized by both high reverberation levels and low SIR. The results for this subset confirm that iCOSPA beneficially uses the DoA information for finding the correct target speaker. Furthermore, it can be seen that employing the 3D convolutional layer in the CRUNet consistently increases the performance of iCOSPA on the *ws* subset. The results on the *cs* subset show that iCOSPA-mvdr-2D and iCOSPA-mvdr outperform COSPA-mvdr even when COSPA chooses the correct speaker for extraction. This indicates that the more precise spatial filtering due to the added DoA information improves overall performance. The differences in performance between iCOSPA-mvdr-2D and iCOSPA-mvdr are not as consistent as for the *ws* subset, which suggests that employing the 3D convolutional layer in the CRUNet is especially beneficial in challenging scenarios. We also investigated the robustness of iCOSPA to DoA-estimation errors, given that in a real scenario the exact DoA might not be available. Adding uniformly sampled estimation noise from -10° to 10° to the true DoA in testing does not notably influence the performance of iCOSPA.

For the comparison to the EaBNet, we look at the networks trained on the mic1-target and focus on the comparison to COSPA, since the EaBNet also does not know which speaker to extract. For the metrics based on the dry reference signal, COSPA-mic1 outperforms the EaBNet, while for the metrics based on the reverberated reference signal the EaBNet outperforms COSPA in terms of Δ PESQ and Δ SIR. The effect of the reference for the metrics on the evaluation is clearly noticeable here. iCOSPA-mic1 outperforms the EaBNet for all metrics. Interestingly, the OMVDR BF outperforms iCOSPA in terms of Δ ESTOI and the dry-reference Δ SIR but not in terms of Δ PESQ. According to listening tests, iCOSPA manages better to actually suppress the interfering speakers, while the OMVDR BF rather elevates the target speaker.¹ In conclusion, including the DoA information into the network indeed helps iCOSPA to identify the correct target speaker and leads to good TSE performance.

3.2.2. Influence of training target on spatial filtering

Building on the discussion of training targets for spectro-spatial filtering in Sec. 2.2, Fig. 3 shows exemplary beampatterns for iCOSPA. It can be seen that the beampattern for the network trained on the MVDR BF-filtered signal shows the most pronounced and precise beampattern. The DSB-filtered target also leads to a distinct beampattern, which indicates that the network is able to learn the spatial selectivity patterns imposed on the target signals in the case of the

¹Upon publication, audio examples will be provided at <https://github.com/LMSAudio/>.

Table 1: Performance metrics for TSE. Metrics are presented with the *dry/reverberated* source signals as references. The best value per metric is printed in bold, the best value per group is underlined.

Model	# Param. [million]	Δ PESQ	Δ ESTOI	Δ SIR [dB]
OMVDR BF	-	0.21/0.32	0.19/0.10	9.71/8.70
EaBNet-mic1 [7]	2.8	0.12/0.30	0.05/0.05	5.88/8.03
COSPA-mvdr	2.1	<u>0.20/0.22</u>	<u>0.12/0.02</u>	8.12/6.75
COSPA-dsb	2.1	0.19/ <u>0.29</u>	0.09/ <u>0.05</u>	6.86/ <u>7.28</u>
COSPA-mic1	2.1	0.14/0.25	0.07/ <u>0.05</u>	6.39/7.22
COSPA-dry	2.1	<u>0.20/0.07</u>	0.11/- 0.02	<u>8.61/6.38</u>
iCOSPA-mvdr	2.6	0.23/0.27	<u>0.14/0.05</u>	8.82/7.59
iCOSPA-dsb	2.6	0.20/0.34	0.11/0.07	7.54/8.24
iCOSPA-mic1	2.6	0.19/ 0.36	0.10/ <u>0.08</u>	7.28/ 8.99
iCOSPA-dry	2.6	0.23/0.08	0.13/- 0.01	<u>9.63/7.08</u>
COSPA-mvdr <i>cs</i>	2.1	0.22/0.24	0.13/0.03	10.44/10.75
iCOSPA-mvdr-2D <i>cs</i>	2.5	0.23/0.25	<u>0.15/0.05</u>	<u>11.32/11.85</u>
iCOSPA-mvdr <i>cs</i>	2.6	<u>0.24/0.29</u>	<u>0.15/0.05</u>	11.09/11.59
COSPA-mvdr <i>ws</i>	2.1	-0.01/- 0.05	-0.04/- 0.11	3.32/3.36
iCOSPA-mvdr-2D <i>ws</i>	2.5	0.06/0.07	0.04/ <u>-0.03</u>	6.63/6.75
iCOSPA-mvdr <i>ws</i>	2.6	<u>0.07/0.11</u>	<u>0.05/-0.03</u>	<u>6.87/6.96</u>

two beamformers. As can be seen in Fig. 3c, using the desired signal at the first microphone as training target also leads to spatial awareness but with less suppression in the non-target directions, while the beampattern of the network trained on the dry source signal shown in Fig. 3d reflects the spatial awareness of the two beamformer-filtered signals with stronger overall suppression. The attenuation in Fig. 3d is due to the more aggressive filtering required to suppress the reverberation to attain the dry source target. Comparing the beampattern for COSPA-dry (not shown) and iCOSPA-dry, it can be stated that the beampattern for COSPA-dry exhibits the same general structure as iCOSPA-dry but not as pronounced, i.e., with less strong gradients. Additionally to confirming that the network can learn the spatial selectivity even without the DoA information passed to the network (cf. [6]), this shows that the spatial selectivity can also be achieved without enforcing a specific spatial filtering process by the target signal. The spatial guiding performed in iCOSPA then supports the network to represent an even more effective spatial filter. The less strong suppression for the mic1-target in Fig. 3c could be due to the reverberation contained in the target, which requires signal parts from all directions. In conclusion, the training target not only provides the network with the ideal characteristics of the estimated signal, but also influences the spatial filter represented by iCOSPA.

Table 1 summarizes the performance of COSPA and iCOSPA trained on various target signals. It can be seen that the evaluation metrics vary strongly with the training target and the reference signal for the metrics. For the metrics based on the dry source signal, the networks trained on the first microphone channel perform worst, while the MVDR BF-filtered target and the dry source target compete for the best performance. For the metrics based on the reverberated source signal, the DSB-filtered target and the mic1-target give the best results, possibly because, compared to the other targets, they retain more of the unprocessed reverberation. The listening impression mostly reflects the results presented in Table 1. iCOSPA-mvdr and iCOSPA-dsb generate similar results, while the results from iCOSPA-mic1 preserve more reverberation and with that also more of the interfering signals. The results generated from iCOSPA-dry show the best interferer suppression but also contain some artefacts. This correlates with the strong suppression visible in Fig. 3d. In general, all iCOSPA variants generate very good speech

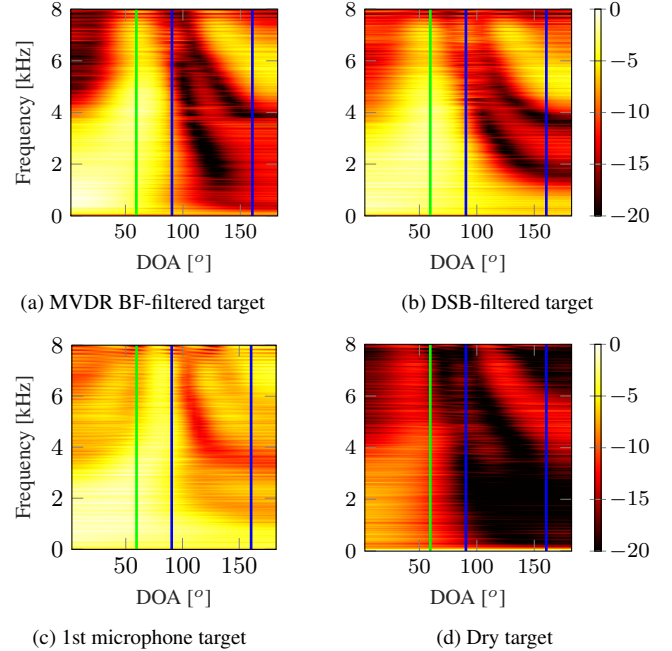


Fig. 3: Exemplary beampatterns for iCOSPA trained on different target signals. green line: target speaker; blue lines: interferers

quality for the target speaker and differ mostly in the suppression of the interferers, which is also reflected in the beampatterns in Fig. 3. The decision on the ‘best version’ will still depend on the scenario, as e.g., for sources close to the first microphone dereverberation will not be as desirable as for distant sources in a highly reverberant room, for which training with clean sources may be preferable.

Finally, in experiments with the EaBNet, some dependency of the spatial selectivity of the network on the target signal can also be observed. This supports the findings that choosing the training target for spectro-spatial filtering impacts not only the performance, but also the interpretability of a method. The generalizability of the results discussed above to other neural network architectures will be addressed in further work.

4. CONCLUSION AND OUTLOOK

In this paper, we presented iCOSPA, an informed extension of COSPA for TSE that exploits additional DoA information. Moreover, we adapted the 2D CRUNet in iCOSPA’s encoder to use a 3D convolutional layer. We showed that iCOSPA uses the provided DoA information to consistently outperform COSPA and to reliably extract the target speaker. The main contributions of this paper are the analysis and interpretation of the influence of the training target on the spatial filtering behavior of iCOSPA, and the demonstration of the impact of the reference signal on the evaluation metrics. We found that the iCOSPA architecture allows to learn beampatterns directed towards the target speaker even if only a dry source signal is used as training target. When using a target signal that results from spatial filtering, this effect is significantly amplified.

A more comprehensive evaluation of the 3D convolutional layer for multichannel audio signal processing is planned for future work. This includes analyzing the effect the 3D processing has on mask estimation in iCOSPA’s encoder, and investigating the impact of equalizing the phase delay between microphones before using the 3D convolutional layer.

5. REFERENCES

- [1] X. Zhang, Z.-Q. Wang, and D. Wang, “A speech enhancement algorithm by iterating single- and multi-microphone processing and its application to robust asr,” in *IEEE Int. Conf. Acoust., Speech and Signal Process. (ICASSP)*, 2017, pp. 276–280.
- [2] Z.-Q. Wang and D. Wang, “All-Neural Multi-Channel Speech Enhancement,” in *Proc. Interspeech 2018*, 2018, pp. 3234–3238.
- [3] J. M. Martín-Doñas, J. Jensen, Z.-H. Tan, A. M. Gomez, and A. M. Peinado, “Online multichannel speech enhancement based on recursive em and dnn-based speech presence estimation,” *IEEE/ACM Trans. Audio, Speech and Lang. Process.*, vol. 28, pp. 3080–3094, 2020.
- [4] Y. Masuyama, M. Togami, and T. Komatsu, “Consistency-aware multi-channel speech enhancement using deep neural networks,” in *IEEE Int. Conf. Acoust., Speech and Signal Process. (ICASSP)*, 2020, pp. 821–825.
- [5] Z.-Q. Wang, P. Wang, and D. Wang, “Complex spectral mapping for single- and multi-channel speech enhancement and robust ASR,” *IEEE/ACM Trans. Audio, Speech and Lang. Process.*, vol. 28, pp. 1778–1787, 2020.
- [6] M. M. Halimeh and W. Kellermann, “Complex-valued spatial autoencoders for multichannel speech enhancement,” in *IEEE Int. Conf. Acoust., Speech and Signal Process. (ICASSP)*, 2022, pp. 261–265.
- [7] A. Li, W. Liu, C. Zheng, and X. Li, “Embedding and beamforming: All-neural causal beamformer for multichannel speech enhancement,” in *IEEE Int. Conf. Acoust., Speech and Signal Process. (ICASSP)*, 2022, pp. 6487–6491.
- [8] Z. Meng, S. Watanabe, J. R. Hershey, and H. Erdogan, “Deep long short-term memory adaptive beamforming networks for multichannel robust speech recognition,” in *IEEE Int. Conf. Acoust., Speech and Signal Process. (ICASSP)*, 2017, pp. 271–275.
- [9] X. Xiao et al., “Deep beamforming networks for multi-channel speech recognition,” in *IEEE Int. Conf. Acoust., Speech and Signal Process. (ICASSP)*, 2016, pp. 5745–5749.
- [10] B. Li, T. N. Sainath, R. J. Weiss, K. W. Wilson, and M. Bacchi-ani, “Neural network adaptive beamforming for robust multi-channel speech recognition,” in *Interspeech*, 2016.
- [11] K. Tan, Z.-Q. Wang, and D. Wang, “Neural spectrospatial filtering,” *IEEE/ACM Trans. Audio, Speech and Lang. Process.*, vol. 30, pp. 605–621, 2022.
- [12] Z.-Q. Wang and D. Wang, “Multi-microphone complex spectral mapping for speech dereverberation,” in *IEEE Int. Conf. Acoust., Speech and Signal Process. (ICASSP)*, 2020, pp. 486–490.
- [13] K. Tesch and T. Gerkmann, “Insights into deep non-linear filters for improved multi-channel speech enhancement,” *arxiv.2206.13310*, 2022.
- [14] K. Tesch, N.-H. Mohrmann, and T. Gerkmann, “On the role of spatial, spectral and temporal processing for DNN-based non-linear multi-channel speech enhancement,” in *Interspeech 2022*, 2022, pp. 2908–2912.
- [15] Z. Chen, X. Xiao, T. Yoshioka, H. Erdogan, J. Li, and Y. Gong, “Multi-channel overlapped speech recognition with location guided speech extraction network,” in *IEEE Spoken Language Technology Workshop (SLT)*, 2018, pp. 558–565.
- [16] R. Gu, L. Chen, S.-X. Zhang, J. Zheng, Y. Xu, M. Yu, D. Su, Y. Zou, and D. Yu, “Neural Spatial Filter: Target Speaker Speech Separation Assisted with Directional Information,” in *Interspeech 2019*, Sept. 2019, pp. 4290–4294.
- [17] K. Žmolíková, M. Delcroix, K. Kinoshita, T. Ochiai, T. Nakatani, L. Burget, and J. Černocký, “Speakerbeam: Speaker aware neural network for target speaker extraction in speech mixtures,” *IEEE Journal of Selected Topics in Signal Processing*, vol. 13, no. 4, pp. 800–814, 2019.
- [18] J. Han, X. Zhou, Y. Long, and Y. Li, “Multi-channel target speech extraction with channel decorrelation and target speaker adaptation,” in *IEEE Int. Conf. Acoust., Speech and Signal Process. (ICASSP)*, 2021, pp. 6094–6098.
- [19] M. Elminshawi, W. Mack, S. Chakrabarty, and E. Habets, “New insights on target speaker extraction,” *arxiv.2202.00733*, 02 2022.
- [20] Y. Hsu, Y. Lee, and M. R. Bai, “Learning-based personal speech enhancement for teleconferencing by exploiting spatial-spectral features,” in *IEEE Int. Conf. Acoust., Speech and Signal Process. (ICASSP)*, 2022, pp. 8787–8791.
- [21] J. H. DiBiase, H. F. Silverman, and M. S. Brandstein, *Robust Localization in Reverberant Rooms*, pp. 157–180, Springer Berlin Heidelberg, Berlin, Heidelberg, 2001.
- [22] P. Pertilä, A. Brutti, P. Svaizer, and M. Omologo, *Multichannel Source Activity Detection, Localization, and Tracking*, chapter 4, pp. 47–64, John Wiley & Sons, Ltd, 2018.
- [23] S. Ji, W. Xu, M. Yang, and K. Yu, “3D convolutional neural networks for human action recognition,” in *Proc. 27th Int. Conf. Machine Learning*. 2010, ICML’10, p. 495–502, Omnipress.
- [24] Ö. Çiçek, A. Abdulkadir, S.S. Lienkamp, T. Brox, and O. Ronneberger, “3D U-Net: Learning dense volumetric segmentation from sparse annotation,” in *Medical Image Computing and Computer-Assisted Intervention (MICCAI)*. Oct 2016, vol. 9901 of LNCS, pp. 424–432, Springer.
- [25] E. Habets, “Room impulse response generator,” Tech. Rep., Technische Universiteit Eindhoven, The Netherlands, 2006.
- [26] J. Garofolo, L. Lamel, W. Fisher, J. Fiscus, D. Pallett, N. Dahlgren, and V. Zue, “Timit acoustic-phonetic continuous speech corpus,” *Linguistic Data Consortium*, Nov 1992.
- [27] ITU-T Recommendation P.862.2, “Wideband extension to recommendation P.862 for the assessment of wideband telephone networks and speech codecs,” Recommendation, ITU, Nov. 2007.
- [28] J. Jensen and C. H. Taal, “An Algorithm for Predicting the Intelligibility of Speech Masked by Modulated Noise Maskers,” *IEEE/ACM Trans. Audio, Speech and Lang. Process.*, vol. 24, no. 11, pp. 2009–2022, Nov. 2016.
- [29] E. Vincent, R. Gribonval, and C. Févotte, “Performance measurement in blind audio source separation,” *IEEE Trans. Audio, Speech and Lang. Process.*, vol. 14, no. 4, pp. 1462–1469, July 2006.